Δελτίο της Ελληνικής Γεωλογικής Εταιρίας τομ. XXXX, 2007
Πρακτικά 11ου Διεθνούς Συνεδρίου, Αθήνα, Μάιος 2007

Bulletin of the Geological Society of Greece vol. XXXX, 2007
Proceedings of the 11th International Congress, Athens, May, 2007

PETROLOGY, GEOCHEMISTRY AND GEOTECTONIC SETTING OF THE TITAROS OPHIOLITE AND ASSOCIATED PELAGONIAN BASEMENT ROCKS IN THE AREA NW OF MT. OLYMPOS, GREECE

Boudi D.[1], Prophitis E.[1], Zachariadis P.[2], Kostopoulos D.[1], Baltatzis E.[1], and Chatzitheodoridis E.[3]

[1] *National and Kapodistrian University of Athens, Faculty of Geology and Geoenvironment, Department of Mineralogy and Petrology, Panepistimioupoli, Zographou, 157 84, Athens, Greece*
boundi.dimitra@hotmail.com, l_profitis@hotmail.com, zacharia@mail.uni-mainz.de, dikostop@geol.uoa.gr, baltatzis@geol.uoa.gr, eliasch@central.ntua.gr

[2] *Johannes-Gutenberg Universität, Institut für Geowissenschaften, Becherweg 21, 550 99, Mainz, Germany*

[3] *National Technical University of Athens, School of Mining and Metallurgical Engineering, Department of Geological Sciences, 9 Heroon Polytechneiou,, Zographou, 157 80, Athens, Greece*

Abstract

The Titaros ophiolite in Greece is a coherent thrust sheet of oceanic rocks that lies atop Permo-Carboniferous granitic orthogneisses and amphibolites of unknown age of the eastern Pelagonian margin in the area NW of Mt. Olympos. It comprises a harzburgite tectonite mantle sequence with chromite mineralisation and a well-developed magma chamber with cyclic units of dunite-lherzolite-wehrlite-pyroxenite that pass upwards into massive gabbros cut by diabase dykes and locally containing plagiogranite ponds. Ophiolite mineral and whole-rock chemistry are strongly in favour of a supra-subduction zone origin in a purely oceanic setting with the occasional brawny signature of melts from subducted sediments. By contrast, the basement amphibolites display a clear within-plate tholeiitic affinity with a slight imprint of subduction-zone fluids. Mineral stretching lineations and kinematics indicators of the orthogneisses and amphibolites suggest a consistent transport direction to the WSW. It is proposed that the basaltic protoliths of the amphibolites were emplaced during Permo-Triassic rifting of the eastern Pelagonian margin that led to the subsequent formation of the Vardar Ocean. The Titaros ophiolite was formed during closure of the Vardar Ocean via northeast-directed intra-oceanic subduction and subsequent obduction towards the southwest onto the eastern Pelagonian margin, probably in the Lower Cretaceous.
Key words: *Wehrlite, rodingite, tawmawite, Raman, supra-subduction zone.*

Περίληψη

Το οφιολιθικό σύμπλεγμα του όρους Τίταρος στην περιοχή ΒΔ του Ολύμπου βρίσκεται επωθημένο σε Περμο-Λιθανθρακοφόρους γρανιτικούς ορθογνεύσιους και άγνωστης ηλικίας αμφιβολίτες στο ανατολικό περιθώριο της Πελαγονικής μάζας. Αποτελείται

από μανδυακό περιδοτίτη χαρτσβουργιτικής σύστασης με κατά τόπους εμφανίσεις χρωμίτη και ένα καλά ανεπτυγμένο μαγματικό θάλαμο με κυκλικές ενότητες σωρειτικών πετρωμάτων δουνίτη-λερζόλιθου-βερλίτη-πυροξενίτη που μεταβαίνουν σε συμπαγείς γάββρους με φωλιές πλαγιογρανιτών και διαβασικές φλέβες στα ανώτερα τμήματά τους. Χημικές αναλύσεις ορυκτών και ολικού πετρώματος φανερώνουν συνθήκες γένεσης του οφιόλιθου σε ένα καθαρά ωκεάνειο περιβάλλον επάνω από μία ζώνη κατάδυσης πλάκας και την περιστασιακή συμμετοχή τηγμάτων προερχόμενων από καταδυθέντα ιζήματα. Οι αμφιβολίτες του κρυσταλλικού υπόβαθρου δείχνουν σαφή χημική συγγένεια προς θολεϊίτες εσωτερικού πλάκας με μια ελαφρά επίδραση από ρευστά καταδυόμενης πλάκας. Εφελκυστικές γραμμώσεις ορυκτών και κινηματικοί δείκτες στους ορθογνεύσιους και αμφιβολίτες υποδηλώνουν φορά μετακίνησης του οφιόλιθου προς τα ΔΝΔ. Προτείνεται ότι οι βασαλτικοί πρωτόλιθοι των αμφιβολιτών τοποθετήθηκαν κατά τη διαμπερή ρήξη του Α. περιθωρίου της Πελαγονικής στο Περμο-Τριαδικό η οποία και κατέληξε στη μετέπειτα δημιουργία του ωκεανού του Βαρδάρη. Ο οφιόλιθος του Τίταρου σχηματίσθηκε όταν ο ωκεανός του Βαρδάρη άρχισε να κλείνει μέσω μιας διαδικασίας ενδο-ωκεάνειας κατάδυσης πλάκας με φορά προς τα ΒΑ και επακόλουθη τοποθέτησή του προς τα ΝΔ επάνω στο Α. περιθώριο της Πελαγονικής, πιθανόν κατά το Κατώτερο Κρητιδικό.
Λέξεις κλειδιά: *Βερλίτης, ροδινγκίτης, τωμωίτης, Ράμαν, ζώνη κατάδυσης πλάκας.*

1. Introduction

In the eastern Mediterranean, the Hellenides of Greece constitute an integral part of the Alpine-Himalayan orogenic system and have traditionally been subdivided into several NW-SE-trending geotectonic zones (Fig. 1). These zones are grouped into two major entities: the External Hellenides, to the west, chiefly composed of non-metamorphosed supracrustal rocks and the Internal Hellenides, to the east, chiefly composed of crystalline basement plus cover units (Papanikolaou 1997). Whereas the External Hellenides represent part of the passive continental margin of the Apulian promontory, the Internal Hellenides represent a mosaic of terranes of Gondwanan origin diachronously accreted to the south-eastern European margin since late Precambrian times (Himmerkus *et al.* 2007, Reischmann and Kostopoulos 2007).

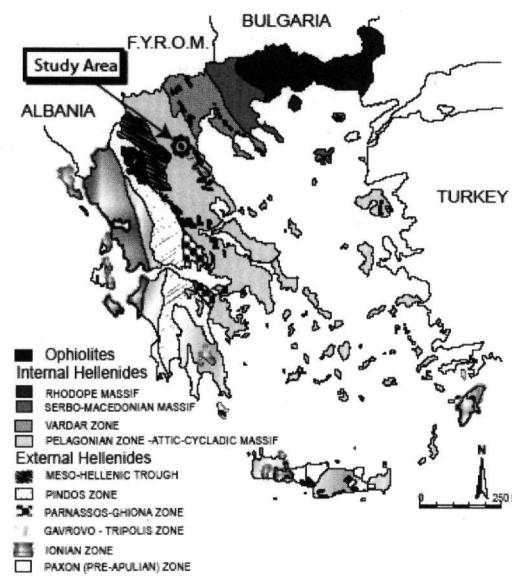

Figure 1 – Geotectonic map of Greece

The Pelagonian Zone belongs to the Internal Hellenides. It is a composite crystalline basement unit composed of Neoproterozoic orthogneisses, paragneisses, schists and amphibolites (Anders *et al.* 2006a) intruded, in turn, by Permo-Carboniferous granitoids (now mostly orthogneisses; Yarwood and Aftalion 1976, Mountrakis 1983, Reischmann *et al.* 2001, Anders *et al.* 2006b) and Permo-Triassic granitoids (Most 2003), and overlain by a Triassic-Jurassic marble cover (see Kilias and Mountrakis 1989, for an overview).

Coherent thrust sheets consisting of ophiolitic rocks occur along the eastern margin of the Pelagonian Zone bordering the Vardar Zone (Nance 1981, Schermer 1993). The latter has long been regarded as the main oceanic terrane of the Dinaric-Hellenic Alps and contains oceanic rocks of upper Middle Jurassic age determined by SHRIMP on zircon separates from plagiogranite pods in upper-level gabbros (Zachariadis *et al.* 2006). Here, we present preliminary results on the petrology, geochemistry and microstructures of the Titaros ophiolite complex and associated basement rocks in the area northwest of Mt. Olympos, Greece.

2. Materials and Methods

For geochemical analyses, the samples were crushed into small pieces and then powdered using an agate mill. Sample powder was mixed with lithium tetraborate (1:7) and fused in platinum crucibles at ca. 1200° C to prepare fused discs. Major-element data were determined by X-ray fluorescence (XRF) on fused discs at the Institut für Geowissenschaften, Mainz, Germany, using a Philips MagiX Pro X-ray spectrometer equipped with an Rh-anode tube. Selected trace elements were analysed using the same analytical equipment but measured on pressed-powder pellets. Relative errors on major and trace elements are usually <2 % and <5 % respectively. Loss on ignition (LOI) was determined gravimetrically by heating the samples to 1000° C. Total iron is expressed as Fe_2O_3. Whole-rock chemical analyses of ophiolitic and basement rocks are tabulated in Table 1.

Mineral analyses were carried out at the Department of Mineralogy and Petrology, Athens, Greece and the Institut für Geowissenschaften, Mainz, Germany. The instrument used in Athens was an EDS Jeol JSM 5600 equipped with an OXFORD LINK ISIS 300 system, and in Mainz a WDS Jeol Superprobe JXA 8900R with ZAF correction provided on-line. The measuring conditions were: beam diameter 2μm, accelerating potential 20 kV, filament current 0.5 nA and counting time 80 s (Athens), and beam diameter 2 μm, accelerating potential 15 kV, filament current 12 nA and counting time 120 s (Mainz). Prior to being loaded into the microprobe, the samples were carbon-coated under vacuum and then degassed for 5 hours in a vacuum chamber.

Laser micro-Raman analyses were conducted at the School of Mining and Metallurgical Engineering, Athens, Greece. Raman spectra were accumulated using a Renishaw 1000 micro-Raman instrument. Excitation was achieved using a HeNe laser (632.8 nm). Forward laser power was 3mW. The laser beam was focused on the sample via a 100x objective lens attached to a metallurgical Leica microscope. Resolution was approximately 2 cm^{-1}.

3. Results and Discussion

3.1. The Titaros ophiolite

3.1.1. General

Detailed fieldwork in the area north of Livadi village has revealed a complete, nearly intact, magma chamber composed of basal dunites overlain by lherzolite-wehrlite-pyroxenite cumulates, in turn overlain by cumulus gabbros that pass upwards into isotropic gabbros which locally contain plagiogranite ponds and are intruded by diabase dykes (Fig. 2). The top part of the magma chamber is abruptly truncated and no contiguous sections of sheeted dykes and pillow lavas were found. The mantle sequence is tectonically detached from the magma-chamber rocks and is composed of harzburgite tectonite with local concentrations of chromite ore. Sheeted dykes and lavas have not been found as yet in the immediate vicinity of the magma-chamber rocks and must have been tectonically transported elsewhere.

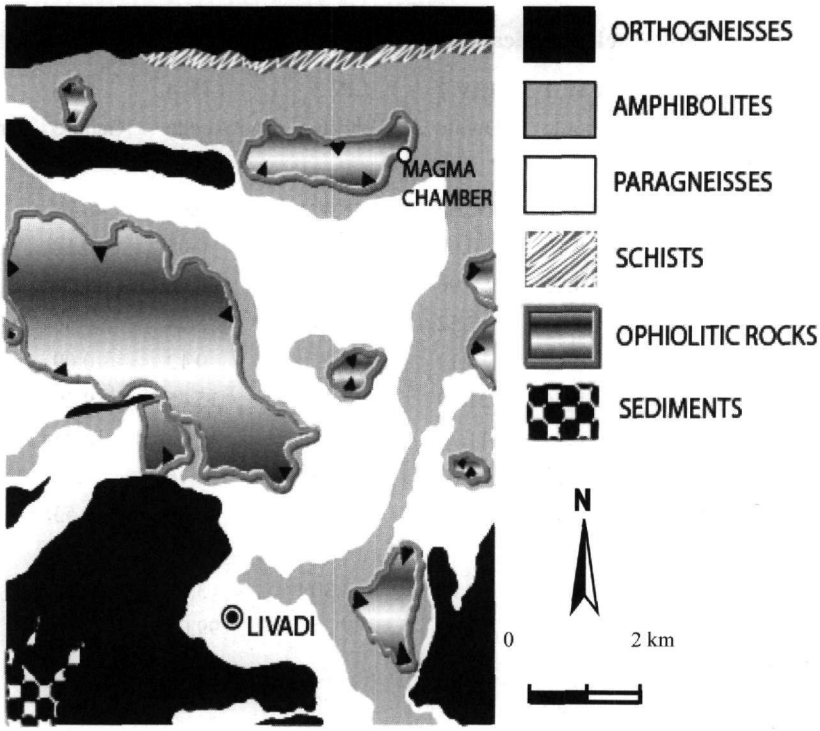

Figure 2 – Simplified geological map of the Titaros ophiolite area

3.1.2. Mineralogy

Primary minerals preserved are olivine and clinopyroxene; spinel has been pervasively transformed to ferritchromite (Table 2). Single-pyroxene thermometry (calibration of Bertrand and Mercier 1985) applied to analysed clinopyroxenes from the wehrlites yielded temperatures in the range 792-987° C for a nominal crystallisation pressure of 2 kb, implying slow cooling of the plutonic sequence, well below the liquidus surface of clinopyroxene. Olivine-spinel thermometry and oxygen barometry (Ballhaus *et al.* 1991 formalism) for the harzburgite tectonites has yielded values of 624° C and $\Delta \log fO_{2(QFM)}$=+6.3 (i.e. Mt-Hm buffer) respectively at a nominal pressure of 5 kb, indicating extensive subsolidus re-equilibration and the prominent effect of serpentinisation.

3.1.3. Metamorphism and laser μ-Raman spectroscopy

All ophiolitic rocks have been metamorphosed under upper greenschist – lower amphibolite facies conditions (500-600° C at P≤5 kb) indicated by the stable coexistence of olivine, serpentine, chlorite, talc and actinolite in the ultramafic lithologies and a clear preponderance of chlorite, actinolite, oligoclase and epidote in the mafic lithologies. It is important to emphasise here the discovery, for the first time in Greece, of Cr-rich epidote – known as tawmawite (Grapes 1981, Treloar 1987, Devaraju *et al.* 1999, Oze *et al.* 2003, Nagashima *et al.* 2006) – in the wehrlites of the cumulate sequence (Table 3). To the best of our knowledge this is the 7th reported tawmawite occurrence in the world. Laser micro-Raman spectra obtained for the first time ever for tawmawite are shown in Figure 3 along with reference epidote spectra. Tawmawite can be distinguished from normal epidote by a well-developed peak of moderate intensity at 831.8 cm^{-1}, four well-developed peaks of moderate and nearly equal intensity at 296.7, 328.6, 350.1 and 392.6 cm^{-1} and by two peaks at 230.3 and 247.0 cm^{-1} that match in intensity the peak at 276.1 cm^{-1}.

Table 1 – Whole-rock chemical analyses of ophiolitic and basement rocks

Sample #	**LIV 1**	**LIV 2**	**LIV 3**	**LIV 4**	**LIV 5**	**LIV 6**
Rock type	Amphibolite	Dunite	Wehrlite	Pyroxenite	Gabbro	Orthogneiss
Major elements (wt%)						
SiO_2	49.20	52.57	48.47	46.64	46.79	76.15
TiO_2	2.10	0.05	0.05	0.05	0.14	0.19
Al_2O_3	14.25	1.96	5.40	9.75	18.71	12.03
Fe_2O_3	11.80	7.52	5.94	5.78	4.66	0.95
MnO	0.17	0.12	0.13	0.12	0.09	0.02
MgO	5.64	21.69	19.03	15.45	9.26	0.15
CaO	8.49	11.71	17.27	17.98	15.25	0.87
Na_2O	4.13	0.03	0.13	0.16	1.12	3.31
K_2O	0.49	0.02	0.02	0.06	0.53	4.42
P_2O_5	0.30	—	—	—	—	0.03
LOI	1.93	3.75	3.30	3.02	2.84	0.77
Total	98.50	99.42	99.74	99.01	99.39	98.89
Trace elements (ppm)						
Sc	30	47	53	57	44	1
V	281	129	154	169	122	9
Cr	141	3109	2630	2163	649	6
Co	48	65	72	52	64	83
Ni	57	531	249	203	143	4
Rb	18	2	4	4	26	102
Sr	177	4	10	80	164	123
Y	43	4	2	3	7	18
Zr	187	17	17	17	18	121
Nb	7	3	3	2	3	10
Ba	27	32	24	39	126	551
Pb	5	—	—	5	13	7
Th	—	—	—	—	—	15.9
U	—	—	—	—	—	4.5
La	11	—	—	—	—	20
Ce	25	—	—	—	—	25
Pr	9	—	—	—	—	—
Nd	16	—	—	—	—	13
Sm	9	—	—	—	—	8
Hf	—	—	—	—	—	—

Table 1 – Whole-rock chemical analyses of ophiolitic and basement rocks (continued)

Sample #	**LIV 7**	**LIV 8**	**LIV 9**	**LIV 10**	**LIV 11**	**LIV 12**
Rock type	Schist	Paragneiss	Gabbro	Amphibolite	Orthogneiss	Dunite
Major elements (wt%)						
SiO_2	59.02	69.45	45.62	50.69	51.85	39.08
TiO_2	0.81	0.62	0.06	1.75	2.83	0.03
Al_2O_3	15.65	11.90	19.51	15.02	12.90	2.85
Fe_2O_3	6.17	4.65	3.04	10.02	12.55	7.30
MnO	0.28	0.09	0.06	0.15	0.23	0.08
MgO	2.06	1.78	10.72	5.35	4.43	38.14
CaO	8.18	3.34	16.17	9.24	4.13	—
Na_2O	3.09	2.46	0.49	2.87	3.84	—
K_2O	1.49	2.27	0.38	0.65	3.36	—
P_2O_5	0.05	0.10	—	0.40	0.53	—
LOI	1.54	1.98	3.41	2.72	2.69	14.02
Total	98.34	98.64	99.46	98.86	99.34	101.50
Trace elements (ppm)						
Sc	17	12	36	30	30	9
V	131	109	77	193	329	53
Cr	215	482	1358	193	111	5747
Co	61	97	61	49	44	61
Ni	7	43	207	55	8	820
Rb	56	87	17	19	215	3
Sr	928	349	109	235	79	4
Y	27	21	3	41	45	2
Zr	160	129	17	234	188	17
Nb	16	11	1	9	9	3
Ba	338	505	86	100	77	15
Pb	77	8	4	4	4	5
Th	8.8	6.7	—	1.6	2.4	—
U	3.9	2.6	—	1.7	—	—
La	24	25	—	15	15	—
Ce	51	40	—	37	41	—
Pr	—	—	—	6	8	—
Nd	27	20	—	27	28	—
Sm	7	5	—	8	11	—
Hf	4.2	—	—	2.9	2.9	—

Table 1 – Whole-rock chemical analyses of ophiolitic and basement rocks (continued)

Sample #	**LIV 13**	**LIV 14**	**LIV 15**	**LIV 16**	**LIV 17**	**LIV 18**
Rock type	Rodingite	Amphibolite	Pyroxenite	Wehrlite	Dunite	Diabase
Major elements (wt%)						
SiO_2	37.84	53.87	43.85	50.97	39.34	46.60
TiO_2	1.01	0.33	0.02	0.06	0.03	0.85
Al_2O_3	27.63	13.05	1.25	2.34	1.33	15.04
Fe_2O_3	5.78	10.69	8.61	5.12	11.60	9.01
MnO	0.08	0.20	0.12	0.14	0.21	0.14
MgO	0.26	7.46	33.30	17.84	35.39	7.54
CaO	23.40	6.44	2.81	20.31	0.04	14.82
Na_2O	—	3.06	—	0.09	—	1.03
K_2O	0.21	1.22	0.01	0.01	—	1.11
P_2O_5	0.05	0.02	—	—	—	0.26
LOI	2.33	2.94	10.61	1.87	12.66	2.72
Total	98.59	99.28	100.58	98.75	100.60	99.12
Trace elements (ppm)						
Sc	26	37	7	63	10	25
V	78	303	38	160	83	140
Cr	88	482	5195	2818	8813	443
Co	46	57	124	54	125	52
Ni	9	128	1543	257	1068	172
Rb	6	39	4	3	4	32
Sr	680	174	8	7	5	1061
Y	79	8	3	3	2	19
Zr	615	37	18	17	17	194
Nb	27	4	2	3	3	14
Ba	103	326	24	34	26	862
Pb	80	8	4	2	3	38
Th	42.6	0.9	—	—	—	12.1
U	5.3	—	—	—	1.7	2
La	135	4	3	—	4	44
Ce	263	—	—	—	—	77
Pr	27	—	—	—	—	13
Nd	114	2	—	—	—	42
Sm	19	—	—	—	—	4
Hf	27	—	—	—	—	2.5

Table 1 – Whole-rock chemical analyses of ophiolitic and basement rocks (continued)

Sample #	**LIV 20**	**LIV 21**	**LIV 22**	**LIV 23**	**LIV 24**
Rock type	Diabase	Harzburgite	Harzburgite	Harzburgite	Amphibolite
Major elements (wt%)					
SiO_2	44.26	42.12	41.86	41.00	50.56
TiO_2	0.32	0.01	0.01	0.01	1.95
Al_2O_3	18.00	0.42	0.40	0.60	14.59
Fe_2O_3	6.70	9.02	8.98	6.78	10.75
MnO	0.11	0.14	0.16	0.10	0.15
MgO	10.98	45.12	45.71	41.89	5.50
CaO	13.01	0.24	0.49	0.01	8.46
Na_2O	0.95	—	—	—	4.21
K_2O	0.40	—	—	—	0.41
P_2O_5	0.02	—	—	—	0.23
LOI	4.14	1.90	1.54	11.75	2.47
Total	98.89	98.97	99.15	102.14	99.28
Trace elements (ppm)					
Sc	36	6	6	7	30
V	126	25	19	23	254
Cr	697	2727	2485	2864	235
Co	57	127	141	99	31
Ni	193	2314	2327	1954	38
Rb	15	3	3	2	15
Sr	117	6	10	4	169
Y	7	3	2	1	35
Zr	33	17	17	16	166
Nb	4	2	3	3	8
Ba	214	28	22	26	14
Pb	4	4	—	2	3
Th	0.2	—	—	—	1.5
U	—	—	—	—	2.2
La	4	—	—	3	11
Ce	4	—	—	—	19
Pr	—	2	—	—	2
Nd	8	—	—	—	16
Sm	6	—	—	—	6
Hf	—	—	—	—	—

LOI: Loss on ignition; —: below detection limit.

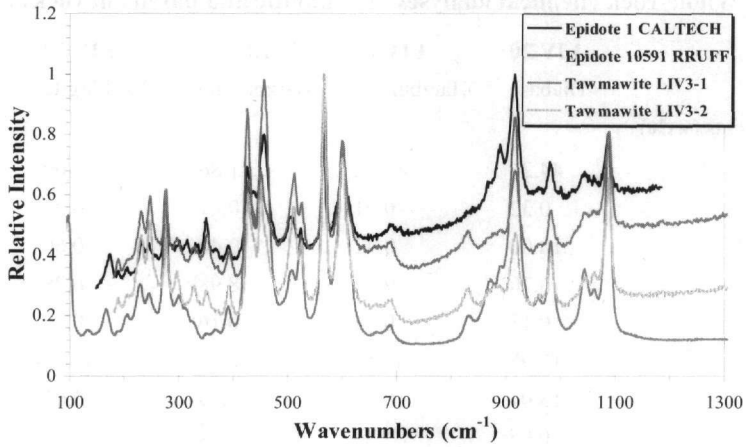

Figure 3 – Laser μ-Raman spectra for tawmawite from the Titaros ophiolite and reference epidote spectra

Worth noting here also is the presence of huge rodingite dykes cutting basal dunites of the magma chamber. They are chiefly composed of clinozoisite / epidote with pumpellyite, titanite, rutile, phengite and zircon occurring as accessories. Pumpellyite is magnesian and slightly zoned with increasing Fe and decreasing Mg content from core (Fe/[Fe+Mg]=0.125) to rim (Fe/[Fe+Mg]=0.152). The pistacite content of the epidote-group minerals also varies considerably between 8.7 mol% in the early clinozoisite and 20.4 mol% in the late epidote associated with pumpellyite formation. The Titaros rodingite is additionally characterised by very low MgO content and very high concentrations of Zr, Nb, Th, U, Pb, Sr, Ba and ΣREE suggesting derivation from a felsic crustal protolith.

Table 2 – Microprobe analyses of clinopyroxene from wehrlite

Sample	**LIV3**	**LIV3**	**LIV3**	**LIV3**
Oxides (wt.%)				
SiO_2	54.36	54.79	56.54	53.56
Al_2O_3	1.73	2.07	1.30	1.75
FeO	3.73	3.74	3.16	3.90
MgO	17.38	17.83	17.61	16.90
CaO	23.27	22.23	23.95	23.62
Cr_2O_3		0.60		0.90
Total	100.47	101.26	102.56	100.63
a.p.f.u. (6 oxygens)				
Si	1.968	1.963	1.996	1.947
Al	0.074	0.087	0.054	0.075
Fe	0.113	0.112	0.093	0.119
Mg	0.938	0.952	0.927	0.916
Ca	0.903	0.853	0.906	0.920
Cr	0.000	0.017	0.000	0.026
Total	3.995	3.985	3.977	4.002
Mg#	0.893	0.895	0.909	0.885
X_{Wo}	0.462	0.445	0.470	0.471
X_{En}	0.480	0.497	0.481	0.469
X_{Fs}	0.058	0.058	0.048	0.061
T (°C)	854	987	861	792

Table 3 – Microprobe analyses of tawmawite from wehrlite

Sample	LIV3	LIV3	LIV3	LIV3	LIV3	LIV3
Oxides (wt.%)						
SiO_2	38.28	39.48	38.80	39.19	39.37	39.08
Al_2O_3	23.79	25.80	25.91	25.40	25.84	25.49
Fe_2O_3	12.72	10.20	11.25	11.58	9.90	10.18
CaO	22.80	23.32	23.09	23.05	23.13	22.49
Cr_2O_3	1.89	2.45	0.66	1.46	2.29	1.31
Total	99.48	101.25	99.71	100.68	100.53	98.55
a.p.f.u. (12.5 oxygens)						
Si	2.997	3.010	3.001	3.009	3.017	3.046
Al	2.195	2.318	2.362	2.299	2.334	2.342
Fe^{3+}	0.750	0.585	0.655	0.669	0.571	0.597
Ca	1.913	1.905	1.913	1.896	1.899	1.878
Cr	0.117	0.148	0.040	0.089	0.139	0.081
Total	7.972	7.965	7.971	7.962	7.961	7.944

3.1.4. Geochemistry and tectonic setting

Petrological types and mineral chemistry (i.e. strongly depleted mantle peridotite, predominance of pyroxenes over plagioclase early in the cumulate sequence, presence of Cr-rich spinel and clinopyroxene in the mantle and the cumulates respectively) suggest formation in a supra-subduction zone setting, similar to that of Pindos (Kostopoulos 1989), Vourinos (Noiret *et al.* 1981, Beccaluva *et al.* 1983, Rassios *et al.* 1983), Troodos (McCulloch and Cameron 1983, Robinson 1983, Cameron 1985, Rautenschlein *et al.* 1985, Bednarz and Schmincke 1994), Oman (Pearce *et al.* 1981, Alabaster *et al.* 1982) and Marum (Jaques *et al.* 1983) ophiolites. This is strongly supported by N-MORB-normalised multi-element profiles for the diabase dykes (Fig. 4), which are typical of those of island-arc tholeiites (Pearce 1982) and boninites, with the occasional strong signature of melts from subducted sediments (Plank and Langmuir 1998). It is proposed that the Titaros ophiolite was formed during closure of the Vardar Ocean via northeast-directed intra-oceanic subduction (see also Stampfli and Borel 2002) and subsequent obduction towards the southwest onto the eastern Pelagonian margin.

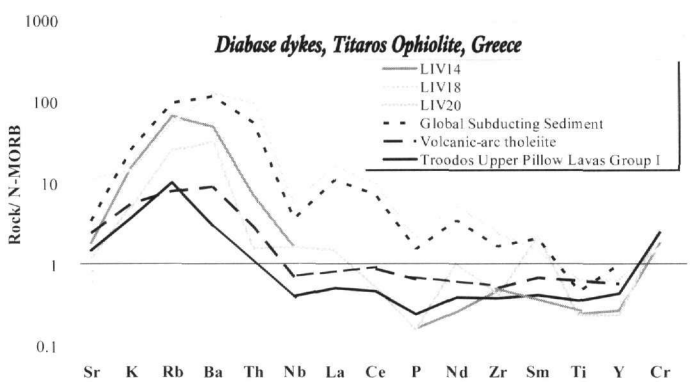

Figure 4 – N-MORB normalised multi-element profiles for diabase dykes of the Titaros ophiolite and reference rocks

With regard to the Pelagonian crystalline basement rocks onto which the Titaros ophiolite was emplaced, the basaltic amphibolites display N-MORB normalised multi-element profiles (Fig. 5)

that are typical of those of within-plate tholeiites (Pearce 1982) and can best be explained by moderate degrees of melting of lithospheric mantle material in the stability field of spinel lherzolite (Kostopoulos and James 1992). These rocks display a slight negative Nb anomaly and it is possible that their source was slightly modified by subduction-zone fluids. This inherited subduction-zone signature in the source region of the amphibolites is tentatively assigned to Permo-Carboniferous subduction of Palaeotethys beneath the southeastern margin of Laurussia that founded the Variscan (Pelagonian) magmatic arc (Stampfli and Borel 2002, Anders *et al.* 2006b). It is then possible that the basaltic protoliths of the amphibolites were emplaced during Permo-Triassic rifting of the eastern Pelagonian margin that led to the subsequent formation of the Vardar Ocean. The granitic orthogneisses show ORG-normalised multi-element profiles (Fig. 6) that match those of volcanic-arc granites (Pearce *et al.* 1984), in full agreement with the extensive results of Anders (2005) and Anders *et al.* (2007, submitted).

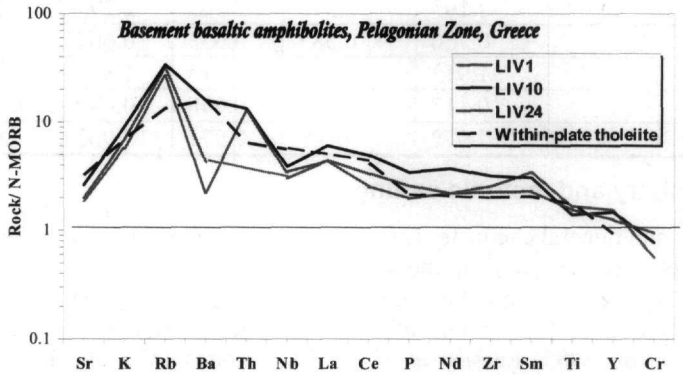

Figure 5 – N-MORB-normalised multi-element profiles for Pelagonian basement amphibolites from the Titaros ophiolite area and reference WPT composition

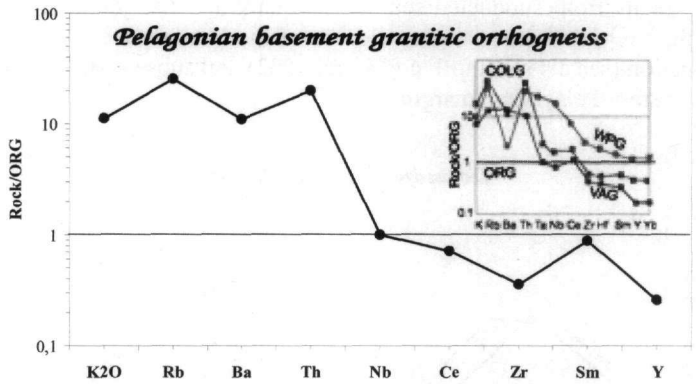

Figure 6 –ORG-normalised multi-element profile for typical Pelagonian basement granitic orthogneiss from the Titaros ophiolite area and reference granite compositions (inset)

3.1.5. Emplacement

A systematic record of mineral stretching lineation and kinematics indicators of the metamorphic basement to the ophiolite thrust sheets (basaltic amphibolites, granitic orthogneisses) suggests a consistent transport direction to the WSW (250°), implying derivation of the ophiolite from an oceanic tract lying to the present ENE of the eastern Pelagonian margin, most probably the Vardar Ocean. Available radiometric data suggest that ophiolite thrusting most probably occurred in the Lower Cretaceous (Yarwood and Dixon 1979).

4. Acknowledgments

Mr. E. Michailidis and Dr. B. Schulz-Dobrick assisted with the microprobe analyses in Athens and Mainz respectively. Ms. N. Groschopf assisted with the XRF analyses in Mainz. We thank the anonymous reviewer for constructive comments. The project is co-funded by the European Social Fund and National Resources – (EPEAEK II) PYTHAGORAS II.

5. References

Alabaster, T., Pearce, J., and Malpas, J., 1982. The volcanic stratigraphy and petrogenesis of the Oman ophiolite complex, *Contributions to Mineralogy and Petrology*, 81, 168–183, 1982.

Anders, B., 2005. The pre-Alpine evolution of the basement of the Pelagonian Zone and the Vardar Zone, Greece, *Unpublished Ph.D. thesis*, Johannes-Gutenberg-Universität Mainz, Germany, 140pp..

Anders, B., Reischmann, T., Kostopoulos, D., and Poller, U., 2006a. The oldest rocks of Greece: First evidence for a Precambrian terrane within the Pelagonian Zone, *Geological Magazine*, 143, 41–58.

Anders, B., Reischmann, T., and Kostopoulos, D., 2006b. Zircon geochronology of basement rocks from the Pelagonian Zone, Greece: constraints on the pre-Alpine evolution of the westernmost Internal Hellenides, *International Journal of Earth Sciences*, DOI 10.1007/s00531-006-0121-7.

Anders, B., Reischmann, T., and Kostopoulos, D., 2007. Geochemistry, tectonic setting and provenance of basement rocks from the Pelagonian Zone, Greece, *submitted.*

Ballhaus, C., Berry, R.F., and Green, D.H., 1991. High pressure experimental calibration of the olivine-orthopyroxene-spinel oxygen geobarometer: implications for the oxidation state of the upper mantle, *Contributions to Mineralogy and Petrology*, 107, 27–40.

Beccaluva, L., Ohnenstetter, D., Ohnenstetter, M., and Paupy, A., 1983. Two magmatic series with island-arc affinity within the Vourinos ophiolite, *Contributions to Mineralogy and Petrology*, 85, 253–271.

Bednarz, U., and Schmincke, H.-U., 1994. The petrological and chemical evolution of the northeastern Troodos extrusive series, Cyprus, *Journal of Petrology*, 35, 489–523.

Bertrand, P., and Mercier, J.–C.C., 1985. The mutual solubility of coexisting ortho- and clinopyroxene: toward an absolute geothermometer for the natural system? *Earth and Planetary Science Letters*, 76, 109–122.

Cameron, W.E., 1985. Petrology and origin of primitive lavas from the Troodos ophiolite, Cyprus, *Contributions to Mineralogy and Petrology*, 89, 239–255.

Devaraju, T.C., Raith, M.M., and Spiering, B., 1999. Mineralogy of the Archean barite deposit of Ghattihosahalli, Karnataka, India, *Canadian Mineralogist*, 37, 603–617.

Grapes, R.H., 1981. Chromian epidote and zoisite in kyanite amphibolite, Southern Alps, New Zealand, *American Mineralogist,* 66, 974–975.

Himmerkus, F., Anders, B., Reischmann, T., and Kostopoulos, D., 2007. Gondwana-derived terranes in the northern Hellenides, *Geological Society of America Memoir*, 200, in press.

Jaques, A.L., Chappell, B.W., and Taylor, S.R., 1983. Geochemistry of cumulus peridotites and gabbros from the Marum Ophiolite Complex, Northern Papua New Guinea, *Contributions to Mineralogy and Petrology*, 82, 154–164.

Kilias, A., and Mountrakis, D., 1989. The Pelagonian nappe: Tectonics, metamorphism and magmatism. Bulletin of the Geological Society of Greece, *23/1,* 29-46 (in Greek with English abstract).

Kostopoulos, D.K., 1989. Geochemistry, petrogenesis and tectonic setting of the Pindos ophiolite, NW Greece, *Unpublished Ph.D. Thesis*, University of Newcastle-upon-Tyne, U.K., 528 pp.

Kostopoulos, D.K., and James, S.D., 1992. Parameterisation of the melting regime of the shallow upper mantle and the effects of variable lithospheric stretching on mantle modal stratification and trace-element concentrations in magmas, *Journal of Petrology*, 33, 665-691.

McCulloch, M.T., and Cameron, W.E., 1983. Nd–Sr isotopic study of primitive lavas from the Troodos ophiolite, Cyprus: evidence for a subduction-related setting, *Geology*, 11, 727–731.

Most, T., 2003. Geodynamic evolution of the eastern Pelagonian Zone in northwestern Greece and the Republic of Macedonia. Implications from U/Pb, Rb/Sr, K/Ar, $^{40}Ar/^{39}Ar$ geochronology and fission track thermochronology, *Unpublished Ph.D. thesis*, Eberhardt-Karls-Universität Tübingen, Germany, 98pp. + Appendices.

Mountrakis, D., 1983. The geological structure of the northern Pelagonian Zone and the geotectonic evolution of the Internal Hellenides. *Habilitation thesis*, Aristotle University of Thessaloniki, Greece, 289 pp. (in Greek with English summary).

Nagashima, M., Akasaka, M., and Sakurai, T. 2006. Chromian epidote in omphacite rocks from the Sambagawa metamorphic belt, central Shikoku, Japan, *Journal of Mineralogical and Petrological Sciences*, 101, 157–169.

Nance, D., 1981. Tectonic history of a segment of the Pelagonian zone, northeastern Greece, *Canadian Journal of Earth Sciences*, 18, 1111–1126.

Noiret, G., Montigny, R., and Allègre, C.J., 1981. Is the Vourinos complex an island arc ophiolite? *Earth Planetary Science Letters*, 56, 375–386.

Oze, C. J., LaForce, M.J., Wentworth, C.M., Hanson, R.T., Bird, D.K., and Coleman, R.G., 2003. Chromium geochemistry of serpentinous sediment in the Willow core, Santa Clara County, CA, U.S. Department of the Interior, U.S. Geological Survey, *Open-File Report 03-251*, 24 pp.

Papanikolaou, D.J., 1997. The tectonostratigraphic terranes of the Hellenides. In D. J. Papanikolaou and. F. P. Sassi (eds), IGCP Project No: 276 Final Volume: Terrane Maps and Terrane Descriptions, *Annales géologiques des pays helléniques*, 37, 495–514.

Pearce, J.A., 1982. Chemical and isotopic characteristics of destructive margin magmas. In R.S. Thorpe (ed.), *Andesites: Orogenic andesites and related rocks*, pp. 525-548, John Wiley and Sons, Chichester.

Pearce, J.A., Alabaster, T., Shelton, A.W., and Searle, M.P., 1981. The Oman ophiolite as a cretaceous arc-basin complex: evidence and implications, *Philosophical Transactions of the Royal Society of London*, Series A 300, 299–317.

Pearce, J.A., Harris, N.B.W., and Tindle, A.G., 1984. Trace element discrimination diagrams for the tectonic interpretation of granitic rocks, *Journal of Petrology*, 25, 956–983.

Plank, T., and Langmuir, C.H., 1998. The chemical composition of subducting sediment and its consequences for the crust and mantle, *Chemical Geology*, 145, 325–394.

Rassios, A., Beccaluva, L., Bortolotti, V., Mavrides, A., and Moores, E.M., 1983. The Vourinos ophiolite complex, *Ofioliti*, 8, 275–292.

Rautenschlein, M., Jenner, G., Hertogen, J., Hofmann, A.W., Kerrich, J., Schmincke, H.-U., and White, W.E.M., 1985. Isotopic and trace element composition of volcanic glass from the Akaki Canyon, Cyprus: Implications for the origin of the Troodos ophiolite, *Earth and Planetary Science Letters*, 75, 369–383.

Reischmann, T., Kostopoulos, D.K., Loos, S., Anders, B., Avgerinas, A., and Sklavounos, S.A., 2001. Late Palaeozoic magmatism in the basement rocks southwest of Mt. Olympos, central Pelagonian Zone, Greece: Remnants of a Permo-Carboniferous magmatic arc, *Bulletin of the Geological Society of Greece*, XXXIV/3, 985–993.

Reischmann, T., and Kostopoulos, D., 2007. Terrane accretion in the internal Hellenides, *Geophysical Research Abstracts*, 9, 05337.

Robinson, P.T., Melson, W.G., O'Hearn, T., and Schmincke, H.-U., 1983. Volcanic glass compositions of the Troodos ophiolite, Cyprus, *Geology*, 11, 400–404.

Schermer, E.R., 1993. Geometry and kinematics of continental basement deformation during the Alpine orogeny, Mt. Olympos region, Greece, *Journal of Structural Geology,* 15, 571–591.

Stampfli, G.M., and Borel, G.D., 2002. A plate tectonic model for the Paleozoic and Mesozoic constrained by dynamic plate boundaries and restored synthetic oceanic isochrones, *Earth and Planetary Science Letters*, 196, 17–33.

Treloar, P.J., 1987. Chromian muscovites and epidotes from Outokumpu, Finland, *Mineralogical Magazine*, 51, 593–599.

Yarwood, G.A., and Aftalion, M. 1976. Field relations and U-Pb geochronology of a granite from the Pelagonian zone of the Hellenides (High Pieria, Greece), *Bulletin de la Société Géologique de France*, 7, 259–264.

Yarwood, G.A., and Dixon, J.E., 1979. Lower Cretaceous and younger thrusting in the Pelagonian rocks of the High Pieria, Greece, *VI^e Colloquium Géologique de Régions Égéenes* (Athens, 1977), 269–280.

Zachariadis, P., Reischmann, T., and Kostopoulos, D., 2006. U–Pb ion-microprobe zircon dating of subduction-related magmatism from northern Greece: The ages of the Guevgueli, Thessaloniki and Chalkidiki igneous complexes, *Geophysical Research Abstracts*, 8, 05560.